

DobLIX: A Dual-Objective Learned Index for Log-Structured Merge Trees

1st Alireza Heidari
Huawei

alireza.heidarikhazaei@huawei.com

2nd Amirhossein Ahmadi
Huawei

amirhossein.ahmadi@huawei.com

3rd Wei Zhang
Huawei

wei.zhang6@huawei.com

Abstract—In this paper, we introduce **DobLIX**, a dual-objective learned index specifically designed for Log-Structured Merge (LSM) tree-based key-value stores. Although traditional learned indexes focus exclusively on optimizing index lookups, they often overlook the impact of data access from storage, resulting in performance bottlenecks. **DobLIX** addresses this by incorporating a second objective, data access optimization, into the learned index training process. This dual-objective approach ensures that both index lookup efficiency and data access costs are minimized, leading to significant improvements in read performance while maintaining write efficiency in real-world LSM-tree systems. Additionally, **DobLIX** features a reinforcement learning agent that dynamically tunes the system parameters, allowing it to adapt to varying workloads in real-time. Experimental results using real-world datasets demonstrate that **DobLIX** reduces indexing overhead and improves throughput by $1.19\times$ to $2.21\times$ compared to state-of-the-art methods within RocksDB, a widely used LSM-tree-based storage engine.

I. INTRODUCTION

Context. key-value (KV) databases are crucial in various domains like cloud computing, e-commerce, big data analysis, and artificial intelligence. Among different KV store architectures, Log-Structured Merge Trees (LSM-trees) stand out for their exceptional write performance [39]. They are widely used in industrial applications, such as RocksDB [17], Cassandra [29], LevelDB [1], and BigTable [10].

The multi-level structure of LSM-trees results in significant drops in read performance due to high read amplification [21], [36]. The levels are divided into Sorted String Tables (SSTables) that contain KV pairs ordered by keys, with SSTables comprising fixed-size blocks (ranging from $4KB$ to $32KB$), and retrieving a specific KV pair involves an index lookup to locate the relevant level, file, block, and pair, followed by a data-access phase to load the block and fetch the desired pair. In current KV stores, with modern NVMe storage, both index lookup and data access contribute significantly to query latency (Fig. 1a).

A common strategy to improve index lookup involves using Machine Learning (ML) as a data structure, effectively revolutionizing data indexing by leveraging predictive capabilities and efficiently capturing records distribution patterns [16], [18]–[20], [23], [24]. This is known as a learned index (LI). These LI models usually reside inside memory and estimate the probable range containing a specific record by evaluating the target key through a monotonic function approximated by a cumulative distribution function (CDF) [22], [34], [40]. However, when

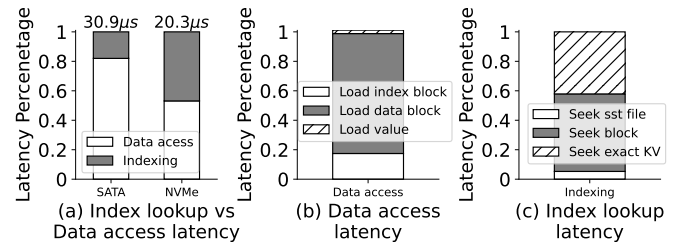


Fig. 1: Lookup Latency Breakdown. Read performance on 10 million 8-byte KVs of the Wiki dataset using the native RocksDB index.

KV pairs are stored in storage, the LI bottleneck emerges during the data retrieval process from storage to memory [30], [35], [48], [53] (§ II-B). Consequently, to overall enhance performance, it is essential to take into account these effective factors.

Current LSM Learned Index Research. The potential enhancement of LSM-tree lookup performance through LI integration has been a focal point in recent studies such as *TridentKV* [36], *Bourbon* [15], *LeaderKV* [47], and *LearnedKV* [45]. These initiatives have introduced customized LI solutions for LSM-tree structures, showing performance gains in index lookup efficiency. A significant oversight in these endeavors is the disregard for data access overhead, especially the time-consuming retrieval of blocks from storage to memory, as shown in Fig. 1b, which leads to a dilemma depicted in Fig. 2 when previous methodologies neglect this characteristic: (1) adhering to fixed block sizes optimized for read operations, which can result in inaccuracies in block lookup and require accessing multiple blocks during read processes. Solutions *a* and *b*, as depicted, face this challenge, a methodology also used by *Bourbon* and *LearnedKV*; (2) Opting for variable block sizes, which could lead to significantly larger blocks, thus increasing block I/O time. Solution *c* exhibits this issue, a methodology also adopted by *TridentKV* and *LeaderKV*. These dilemmas arise from the isolated optimization of LI models without considering the data access component. Consequently, while these techniques reduce average latency compared to LSM tree-based KV store index lookups, they show higher tail-latency in cases requiring multiple or large block retrievals. This paper proposes a new LI solution to optimize both the indexing and data access phases.

Furthermore, earlier studies have neglected the consideration of varying key lengths in their design (§ II-C), as well as the enhancement of the last mile search, which is the final phase to

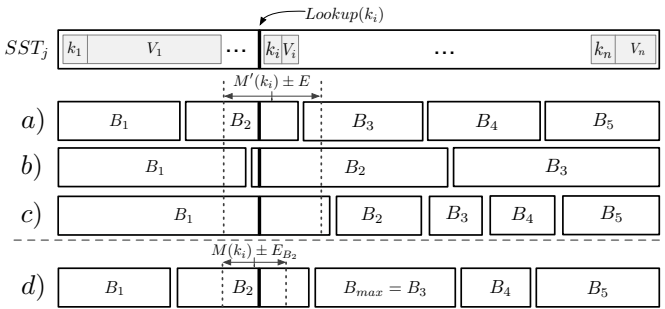


Fig. 2: Comparison of LI Solutions on SSTables. Considering Block Sizes Par_{Block} and the LI $I_{IndexBlock}$ as stochastic variables. **a)** Small fixed-size blocks, **b)** Large fixed-size blocks with a guarantee on max block size. **c)** Variable block size with a model output ($M'(k)$) guarantee to load one block. **d)** Perfect solution with guarantees on model output ($M(k)$) for one block access with optimized block size.

identify the target KV within the retrieved block. As shown in Fig. 1c, this step in the indexing process incurs nearly identical latency to block finding. Therefore, an LI methodology should incorporate optimizations for this critical step.

Our Approach. We leverage multi-objective optimization techniques to incorporate data access overhead as an additional factor to design an LI framework [8]. To achieve a suitable configuration that optimizes index performance alongside this additional parameter, we employ an auto-tuning method based on reinforcement learning (RL). This enables us to develop configurations that generate index models capable of automatically adjusting when workloads change. Our approach specifically concentrates on constructing an index model for KVs at the LSM file level, allowing for **effective locating** of the desired **variable-size** KVs using merely **a single block** access with **ideal block size**, all while maintaining the LI model optimal performance.

We evaluate our framework using an array of real-world and synthetic datasets and workloads, showing a substantial reduction in indexing costs when measured against state-of-the-art indexing solutions. We show that our framework leads to better performance, with throughput improvements between 1.19× and 2.21× in various datasets and workloads.

Technical Challenges. Our approach needs to address multiple technical challenges:

- **Index Model.** Considering a secondary parameter makes the learning of index modeling challenging. The model should consider both parameters during the optimization process, while depending on the type of the second parameter, the cost feedback might come asynchronously.
- **Restoration.** During LSM tree query processing, data spans storage layers with varying performance. Missing metadata (e.g., the “index trajectory”) can disrupt queries and require costly recovery. To avoid this, index system must preserve critical metadata to efficiently handle gaps and ensure smooth query execution.
- **Adaptation.** In an index framework, the parameters of the system can change due to the behavior of the incoming data or workload shifts. The design must adapt to these changes to ensure efficient performance under varying conditions.

Implementing the framework within an LSM-tree-based KV store and conducting comprehensive benchmarking present challenges, primarily due to the incompatibility of many LI models with LSM trees, as well as the inadequacies of current benchmarks (e.g., YCSB) in capturing important edge cases.

Contributions. We present the following contributions in this paper:

- 1) **Proposing *DobLIX*, a *Dual-objective Learned Index* framework**, for LSM tree-based KV stores (§ III-B). This framework optimizes the performance of the LI lookup while considering any additional secondary objective parameter using two innovative LI approximation models, PLA and PRA (§ III-C). In this work, our design specifically optimizes indexing and data access as a secondary parameter.
- 2) **Optimizing the last-mile search phase** of the lookup process by incorporating the LI model traversal into the last mile search process (§ III-E).
- 3) **Introducing an RL-based agent** to dynamically adjust the indexing and data partitioning parameters in our system and to choose between the PLA and PRA methods (§ III-F).
- 4) **Implementing our method on RocksDB** and performing a comprehensive benchmark to demonstrate its superior performance compared to traditional and LI solutions (§ IV).

Paper Organization. The remainder of the paper proceeds as follows: In § II, we review the background concepts. § III provides a detailed overview of our LI framework design and RL-agent. In § IV, we evaluate our proposed solutions. We discuss related work in § V and summarize key points of the paper in § VI.

II. BACKGROUND

A. Data Management and LSM-tree-based KV Stores

In order to formally define the interpretation of the data management system as random variables illustrated in Fig. 2, it is essential to express these variables through a mathematical formulation [11]. Conducting this first, we know that there are two primary methods to reduce the complexity of big data management: (1) *Data Partitioning* ($Par(\cdot)$): divides given data into smaller partitions. (2) *Indexing* ($I(\cdot, \cdot)$): given partitioned data and a query key, it directly returns a subset of partitions where the target key is stored.

$Par(\cdot)$ is unchanged by the key query, but it is possible to assume its integration with $I(\cdot, \cdot)$ for a given key k . Consequently, for simplicity in notation during the construction phase, we can represent it as $I(\cdot)$. This approach lays the foundation for the formation of a comprehensive set of data structures with indexed entries relevant to any dataset D . A general combination form is generated by a set of $\mathcal{P} = \{Par_1, Par_2, \dots, Par_n\}$ and $\mathcal{I} = \{I_1, I_2, \dots, I_m\}$, denoted $\mathcal{F} = f_1(f_2(\dots f_k(D))) = f_1 \circ f_2 \circ \dots \circ f_k(D)$, where f_i belongs to \mathcal{P} for i within the range $[1 : n]$ or to \mathcal{I} for i within the range $[1 : m]$. Recognize that this general structure may imply an infeasible data structure because particular partitions Par_i

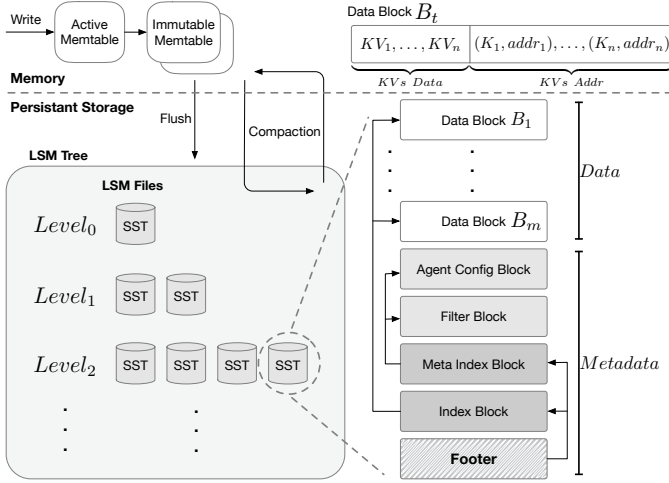


Fig. 3: RocksDB Architecture.

or indexing I_i presume certain data property assumptions about their input arguments. Once the construction is complete, $\mathcal{F}(k)$ acts as the top-level index for the newly built data structure.

In the context of an LSM-tree, the data structure is constructed from four distinct partitions defined as $\mathcal{P}_{LSM} = \{Par_{TreeLevel}, Par_{SST}, Par_{Block}, Par_{KV}\}$. Its indexing mechanism is represented by $\mathbf{I}_{LSM} = \{I_{LevelBloomFilter}, I_{SST}, I_{IndexBlock}, I_{KV}\}$. The composite function is articulated as $\mathcal{F}_{LSM} = I_{KV} \circ Par_{KV} \circ I_{IndexBlock} \circ Par_{Block} \circ I_{SST} \circ Par_{SST} \circ I_{LevelBloomFilter} \circ Par_{TreeLevel}(D)$.

Breaking down \mathcal{F}_{LSM} , initially, the given data D is partitioned into a hierarchical structure through tree levels ($Par_{TreeLevel}$), employing a level bloom filter ($I_{LevelBloomFilter}$) that generates a Boolean index indicating the presence of a key at a particular level. Within each level, data are segregated into distinct SST files (Par_{SST}) with an index that maintains the key range within each SST and uses linear search, acting as the SST index (I_{SST}). Each SST arranges data in a sorted manner and is further divided into uniform blocks (Par_{Block}) containing key-value pairs (Par_{KV}). Furthermore, each SST contains an index block as part of its metadata, which includes an index entry for every data block ($I_{IndexBlock}$) facilitated by binary search, along with KV pairs indexed by I_{KV} that are subjected to linear search in RocksDB. Fig. 2 demonstrates four different Par_{Block} configurations {a,b,c,d}, each generating a unique block-level division within the same SST file; further details are provided in § III-B.

B. Learned Index (LI)

Learned indexes [16], [18], [27], [32], [42] aim to improve the efficiency of data retrieval in database systems by employing machine learning models to map keys to their respective locations. These indexes can involve intricate models, such as neural networks, or simpler hierarchically organized models, such as linear models. Traditional LIs use ensemble learning and hierarchical model structuring. Starting from the root node and progressing downward, the index model $I(k)$ predicts

the subsequent layers to utilize for a query key k based on $I(k) = M(k) \times N$, where N represents the number of keys, and M denotes the cumulative distribution function (CDF) that estimates probability $p(x \leq k)$. Given the complexity of training and inference in sophisticated models, many LIs adopt piecewise linear models to approximate the CDF. Querying entails predicting the key position using $pos = a \times k + b$ with a maximum error e , where a and b are learned parameters, and e is crucial for the final search to locate the target key. These indexes exhibit memory efficiency because of their lightweight parameters (an intercept along with a likely slope) compared to conventional indexes.

1) **LI on Persistent Storage:** Recent studies [30], [35], [48], [53] have shown that current LIs do not outperform traditional index solutions like B+tree when KVs reside within persistent storage. These studies highlight that the design of LIs fails to leverage the characteristics of disk storage, necessitating multiple disk I/O operations during the last-mile search process as shown in Fig. 4. A similar trend is observed in LI techniques for LSM-trees, which also entail substantial I/O operations during their final search phase. This underscores the importance of considering I/O as a critical element in the development of LI systems.

2) **LI on Strings:** The exploration of LIs has predominantly revolved around fixed-sized integers or floating-point keys. However, their application to variable-length string keys has received relatively less attention, with only a few studies addressing this issue [41], [46], [51]. An advanced solution in this domain is the Radix String Spline (RSS) [41], which employs a trie-based approach. In RSS, each trie node handles 8-byte or 16-byte keys and computes a Radix Spline (RS) model [27] for these keys. The memory architecture and the programming language used typically impose limits on the size of integer types. In a 64-bit memory environment, the largest standard integer type that C++ natively supports is `__uint64_t`. However, some compilers provide non-standard support for 128-bit integers (e.g. `__uint128_t`), which can be effectively utilized to convert a Trie tree node from a string format to an integer representation. The RS model, a piecewise linear model, provides monotonic CDF predictions within a specified error threshold. For keys that exceed the error limit (e.g. due to shared prefixes), RSS stores the key in a redirector map and creates a new child node for that key. RSS compares 8-byte or 16-byte segments of keys, incurring lower costs compared to full-key comparisons. Despite these relatively small comparisons, the last-mile search process remains costly. A recent study [51] indicates that RSS spends more than 70% of its time in the last-mile search phase, which points to significant optimization potential in the last-mile search for LIs on string keys.

C. Key-Value Length in LSMs

LSM-tree storage engines are commonly used in various applications and services, including social networks, financial systems, and AI workflows. Thus, they need to handle keys

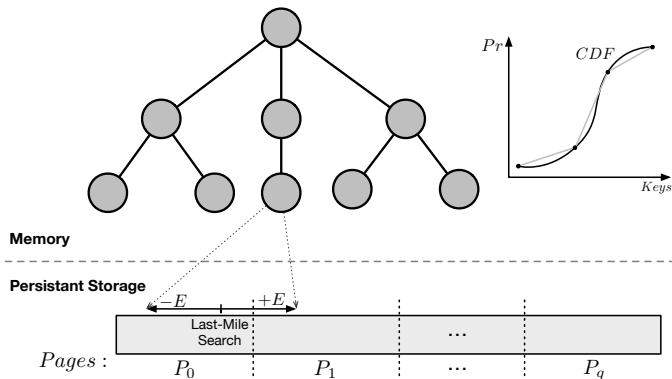


Fig. 4: LI on Persistent Storage. The model last-mile search range may require loading multiple pages from the storage.

TABLE I: AVG and SD of key-values (in bytes) on RocksDB use cases on UDB, ZippyDB, and UP2X.

Application	Key		Value	
	AVG	SD	AVG	SD
UDB	27.1	2.6	126.7	22.1
ZippyDB	47.9	3.7	42.9	26.1
UP2X	10.4	1.4	46.8	11.6

and values of all types and lengths. The study by Cao et al. [9] examines the use of RocksDB in three different use cases at *Meta* (see Table I): **UDB** (storage engine of a SQL database), **ZippyDB** (storage engine of a distributed KV-store), and **UP2X** (persistent storage of an AI/ML service). The study presented the average (AVG) and standard deviation (SD) of the KV length in these applications. Both keys and values were found to have variable sizes, with a smaller standard deviation for keys and a larger for values. Previous LSM-tree LI solutions [15], [36], [45], [47] are limited to fixed key sizes, rendering them unsuitable for these applications.

D. Lexicographic Optimization

Lexicographic optimization [7], [12] is a structured approach to solving multiobjective optimization problems by prioritizing objectives based on their importance. The highest priority objective is optimized initially, followed by the next objectives, within a feasible space that preserves the previously achieved optimizations. This method ensures that each objective is tackled sequentially according to its rank, ensuring that earlier optimizations remain unaffected by appropriately constraining the subsequent optimization problems. This method simplifies decision-making policy of exploration in feasible space with a clear hierarchy by addressing the objectives one at a time. It offers a deterministic way to handle multiple objectives, which is useful for non-negligible goals in resource allocation or scheduling. By prioritizing critical objectives, lexicographic optimization ensures that they are met without compromise, allowing secondary goals to be optimized within the feasible solution space.

III. DOBLIX DESIGN

In this section, we describe how **DobLIX** is designed to speed up lookup queries. We first dive into the general

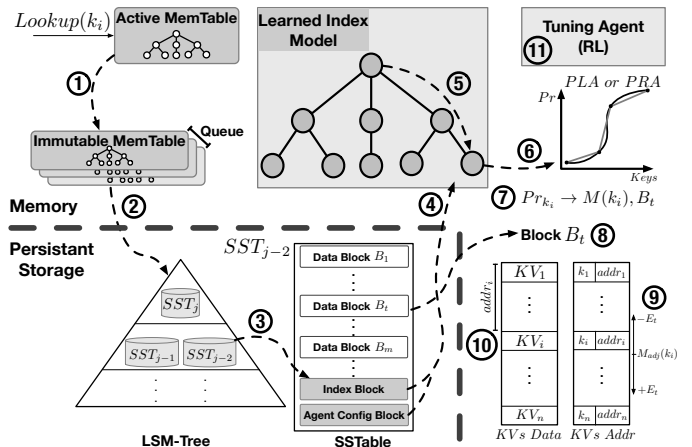


Fig. 5: **DobLIX** Architecture.

architecture and core concepts of **DobLIX** (§ III-A and § III-B). To align index modeling with dual objectives, **DobLIX** utilizes two LI approaches: it modifies the existing Piecewise Linear Approximation (PLA) method [27] by adjusting the spline operations to incorporate new objective functions, and introduces a novel indexing strategy called Piecewise Regression Approximation (PRA), which improves performance by effectively managing modeling errors (§ III-C). **DobLIX** incorporates a string-compatible LI solution capable of handling variable-size KVs. To optimize the last-mile search process, it transfers model knowledge to narrow the search range and simplifies key comparisons by focusing solely on a limited part of the key bits decodable as an integer (§ III-E). Furthermore, it utilizes a reinforcement learning (RL) tuning agent to dynamically determine optimal parameters, such as the maximum approximation error of the allowed model and block size, and to select between the PLA and PRA algorithms (§ III-F).

A. Overall Architecture

Fig. 5 outlines the general architecture of **DobLIX**. This solution concentrates on learning the index at the SSTable level in detail. SSTables are preferred for LIs due to their unchanging nature, which removes the need for updates during their lifespan. Upon the formation of each SSTable, **DobLIX** trains an LI model based on its KVs. This model is crafted to accurately pinpoint the target block for all KVs within a specified error margin while ensuring that block sizes remain within the designated maximum limit. Consequently, **DobLIX** has an LI model and block partitioning, as illustrated in Fig. 2d. Subsequently, **DobLIX** serializes the LI model and deposits it in the index block within the SSTable metadata.

Lookup Process. In Fig. 5, the stages involved in a **DobLIX** lookup query are outlined. ① Initially, it inspects the current MemTables; if the desired key is absent there, it looks through the unalterable MemTables. ② It then scrutinizes various levels of LSM-trees and ③ loads the SSTable that may cover the target key within its range. ④ **DobLIX** loads the LI model from the SSTable metadata into memory. ⑤ It performs a search within its Trie tree to locate the node that houses the ultimate LI

(§ II-B2) and ⑥ uses the trained CDF model within that node to ⑦ determine the **exact block number** that contains the key and **narrows down the search scope** for the last-mile search in the block using the LI model. ⑧ Following this, `DobLIX` loads the block from storage in memory and ⑨ executes the final search within the specified range in $KVs\ Aaddr$ stored in the blocks' metadata to find the exact offset of the target KV pair in the $KVs\ Data$ (§ III-E), and ⑩ employs the retrieved address on the $KVs\ Data$ to locate the actual KV. ⑪ Finally, `DobLIX` measures the *latency* of the current lookup query alongside the *index size*, incorporating these measurements as feedback to refine the tuning agent (§ III-F).

B. Concept Overview

The management of LSM-tree data involves data partitioning and indexing phases (§ II-A), and as we established earlier, any optimization strategy, especially those involving LIs, should improve overall performance. As depicted in Fig. 2, block partitioning is intertwined with block indexing ($Par_{Block} \nleftrightarrow I_{IndexBlock}$). Therefore, optimizing $I_{IndexBlock}$ requires the consideration of Par_{Block} . In contrast, previous designs illustrated in Fig. 2{a,b,c} from earlier research have significant data access expenses due to the independence between the LI model and the data partitioning component. As described in § II-B, within the traditional framework of LI modeling, $I(\cdot)$ represents the result of approximating keys indexes drawn from an unknown distribution \mathcal{D}_{keys} through practical optimization. Therefore, the classical design of the LI does not consider data access and the result coordinated by all data; however, in LSM-trees only a limited number of SSTable blocks reside in memory. In addition, the primary optimization objective is to minimize the error within the hypothesis spaces chosen, regardless of any secondary objectives.

`DobLIX` aims to redefine LI models by integrating efficient block-based data access as a key objective. Enhances indexing performance by ensuring that the trained model accurately maps queries to the correct block, enabling the retrieval of only a single block while adhering to the optimal block size. A critical aspect of `DobLIX` is the relationship between the index approximation ($I_{IndexBlock}$) and block partitioning (Par_{Block}), where a one-to-one correspondence is established between the index approximation and the segments within Par_{Block} . This allows `DobLIX` to apply LI models that partition the key domain into segments, ensuring each segment corresponds to a specific block. The system performs a binary search on an array of offsets ($I_{IndexBlock}$) to find the start of each segment (i.e. block). Within each segment, it uses an index approximation (I_{KV}) to efficiently locate the keys. Since the trained index is based on the entire data in SSTable, the index model used for each block requires adjustment (§ III-E). This approach optimizes both block access and key retrieval, providing efficient indexing.

To achieve this, we introduce a dual-objective optimization approach for two distinct LI methodologies. The first method is based on the piecewise linear approximation (PLA) modeling [27], while the second method employs the piecewise

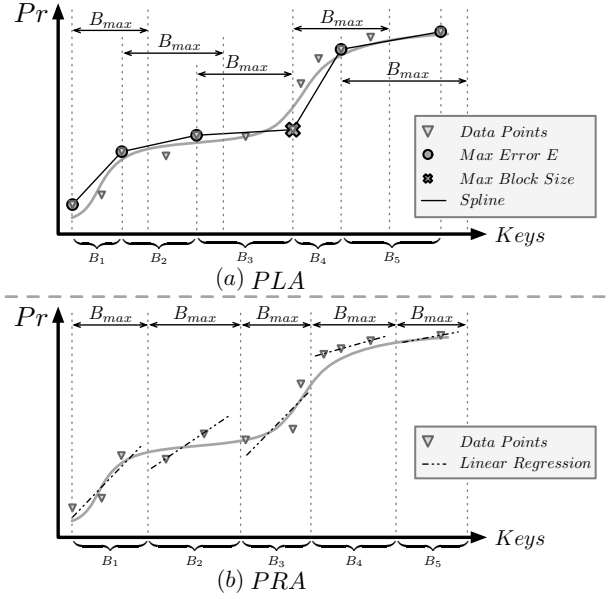


Fig. 6: LI Models. B_i s represent the actual blocks added to SSTables.

regression approximation (PRA), based on the recursive model index [28]. We delve into these methods in § III-C2 and § III-C3.

C. LI Approximation Methods

In this section, we present our LI algorithms that focus on dual-objective optimization to train the index model. Considering the importance of I/O performance in indexing, these algorithms are designed to partition the KV space based on their sizes and progressively systematically construct the index. Typically, we approximate the index for each segment using linear models. When it comes to searching for specific points during lookup processes, we employ a binary search on the points derived from the piecewise approximation to precisely pinpoint the required location, which is referred to as last-mile search. In the following, we elaborate on these algorithms in detail.

1) **Dual-Objective Optimization:** To address both the data access and index approximation goals, we used lexicographic optimization (§ II-D). As demonstrated by the motivational experiment in Fig. 1a, data access significantly influences latency performance. Although various methods exist to tackle multi-objective optimization problems, we aim to prioritize the data access parameter more heavily than index lookup. Thus, we always finalize a block when its size exceeds the maximum block size B_{max} by incorporating an additional pair of key values. This ensures that the block sizes remain below B_{max} , even if the approximation error E has not yet been achieved. Note that both the configuration values B_{max} and E are given by the *Tuning Agent* (§ III-F).

2) **Piecewise Linear Approximation (PLA):** In this method, the key space is divided into blocks B_i using a linear approximation (spline), each block containing keys that share a common prefix. For each block B_i , a spline estimate of the positions is made, defined as $M_i(x) = a_i + b_i(x - x_i)$, where a_i

Algorithm 1: Dual-objective PLA

Input: Set of KVs D
Output: Radix Points \mathcal{R}

```
1  $\mathcal{R} \leftarrow []$ ,  $index \leftarrow 0$ ,  $offset \leftarrow 0$ 
2  $E, B_{max} \leftarrow TuningAgent()$ 
3  $B_{curr} \leftarrow [(k_0, v_0)]$ 
4 while  $(k, v) \in D$  do
5   if  $|B_{curr}| > B_{max}$  then
6      $\mathcal{R} \leftarrow \mathcal{R} + [B_{curr}.last]$ 
7      $B_{curr} \leftarrow [(k, index)]$ 
8   if  $|B_{curr}| >$ 
9      $1 \wedge APE(Line(B_{curr}.first, (k, index)), B_{curr}) \geq E$ 
10    then
11       $\mathcal{R} \leftarrow \mathcal{R} + [(B_{curr}.last, offset)]$ 
12       $offset \leftarrow offset + |B_{curr}|$ 
13       $B_{curr} \leftarrow [(k, index)]$ 
14    else
15       $B_{curr} \leftarrow B_{curr} + [(k, index)]$ 
16     $index \leftarrow index + 1$ 
17  $\mathcal{R} \leftarrow \mathcal{R} + [(B_{curr}.last, offset)]$ 
```

and b_i are coefficients derived from control points and x_i is the initial key in block B_i . The binary search is then used around $M_i(k)$ to identify the precise index $I(k)$. For each block B_i , the next key is added to a new block (B_{i+1}) of the SSTable if (1) the approximation error $M_i(x)$ reaches the maximum threshold E , or (2) the condition $|B_i| \geq B_{max}$ indicates that including the new pair of KV would exceed the maximum block size allowed. This approximation process is illustrated in Fig. 6a. As described in § III-C1 when the size of an added point exceeds B_{max} , a new block is created to maintain the optimal I/O (data access) performance of the previous block, as indicated by the cross in Fig. 6a. This mechanism results in a new set of spline points, introducing new blocks when the secondary optimization criterion is met, in addition to the standard blocks formed by reaching the maximum approximation error. Algorithm 1 showcases this approach, where $APE(line, set)$ calculates the maximum distance the points in set can have from the given line $line$. In this context, a_i is defined as $\mathcal{R}[i][0][1]$, x_i corresponds to $\mathcal{R}[i][0][0]$, and b_i is calculated as $\frac{\mathcal{R}[i+1][0][1] - \mathcal{R}[i][0][1]}{\mathcal{R}[i+1][0][0] - \mathcal{R}[i][0][0]}$, while the term $offset_i$ refers to $\mathcal{R}[i][1]$.

3) **Piecewise Regression Approximation (PRA):** This approach involves initially dividing the key domain into segments of size B_{max} and then approximating each segment linearly. The maximum approximation error for each segment, E' , is noted and utilized during the last-mile search phase (refer to Fig. 6b). Start scanning the KVs from the beginning; if incorporating the new KV into the existing segment exceeds B_{max} , start a new segment. Algorithm 2 performs this task in one pass, maintaining the integrity of each KV pair.

After partitioning the data using the optimal block size B_{max} , as outlined in Algorithm 3, a new model can be constructed for each partition through a linear approximation. The boundary points are retained for search tasks to determine the appropriate model for lookup queries, and E' is stored in \mathcal{E} , respectively.

Algorithm 2: Partition $Par_B(\cdot)$

Input: Set of KVs D , Maximum Block Size B
Output: Partition \mathcal{P}

```
1  $t, \mathcal{P} \leftarrow []$  &  $offset \leftarrow 0$ 
2 while  $KV \in D$  do
3   if  $|t| + |KV| > B$  then
4      $\mathcal{P} \leftarrow \mathcal{P} + [(t, offset)]$ 
5      $offset \leftarrow offset + |t|$  &  $t \leftarrow []$ 
6    $t \leftarrow t + [KV]$ 
7  $\mathcal{P} \leftarrow \mathcal{P} + [(t, offset)]$ 
```

Algorithm 3: Dual-objective PRA

Input: Set of KVs D
Output: Radix Points \mathcal{R}
Model Sets \mathcal{M}
Maximum Segment Errors \mathcal{E}

```
1  $\mathcal{R}, \mathcal{M}, \mathcal{E} \leftarrow []$ 
2  $B_{max} \leftarrow TuningAgent()$ 
3  $\mathcal{P} \leftarrow Par_{B_{max}}(D)$  ▷ from Algorithm 2
4 while  $Partition\ par \in \mathcal{P}$  do
5   if  $|par| > 1$  then
6      $M \leftarrow LinearRegression(par)$ 
7      $\mathcal{M} \leftarrow \mathcal{M} + [M]$ 
8      $\mathcal{E} \leftarrow \mathcal{E} + [APE(M, par)]$ 
9    $\mathcal{R} \leftarrow \mathcal{R} + [par.frist]$ 
10  $\mathcal{R} \leftarrow \mathcal{R} + [par.last]$ 
```

4) **Comparing PRA and PLA:** In the context of building block approximations, both the Piecewise Linear Approximation (PLA) and the Piecewise Regression Approximation (PRA) rely on the scanning of data, resulting in a linear time complexity of $O(N)$, where N is the number of data points. Each method utilizes closed-form formulas with a time complexity of $O(N)$ for computations within blocks: PLA determines maximum distances, $APE(\cdot, \cdot)$, to construct piecewise linear segments, while PRA computes two-dimensional regression, $LinearRegression(\cdot)$, formulas within blocks.

With respect to space complexity, PLA requires one point per spline segment to be stored since the endpoint of one line serves as the beginning of the next. The distribution of data points influences PLA memory needs; for instance, with a uniform distribution, all data might fit within a single spline (provided its size is smaller than B_{max}), thus minimizing memory usage. In contrast, PRA must store both a point and a slope for each regression line, roughly doubling the memory requirement compared to PLA. The complexity of the number of regressions is $O(\frac{N}{B_{max}})$. Consequently, the memory comparison between PLA and PRA depends on the characteristics of the data: PLA may involve fewer blocks and needs just one point per block (linear segment), whereas PRA has to retain two parameters per block.

When comparing the behavior of PRA and PLA during lookups (⑦ in Fig. 5), determining which method is superior is challenging, often leading to the interchangeable use of algorithms; in particular, we consider two scenarios that contrast

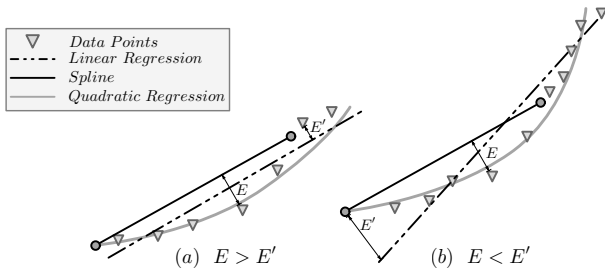


Fig. 7: Comparison of PLA and PRA under different data distributions. (a) $E' < E$, indicating PRA performs better. (b) $E < E'$, indicating PLA performs better.

PLA and PRA, as illustrated in Fig. 7, noting that both scenario (a) and scenario (b) can occur depending on the sizes of the KV pairs and the distribution of the keys. In the PRA model, the block is written in persistent storage once its size reaches the maximum block size B_{max} , whereas the PLA operates under two conditions for flushing: when the approximation error exceeds the error limit E , or when the block size reaches B_{max} (the same maximum block size used in PRA). Consequently, depending on the arrangement and distribution of KV, the spline achievable with PLA can potentially lead to a maximum error E that may be higher or lower than the maximum error E' in PRA. As shown in Fig. 7a, PRA can result in $E > E'$, indicating a more accurate approximation than PLA. This directly affects the scope of the last-mile search and the overall efficiency of each algorithm.

This implies that the behavior of KVs beyond the block boundary determined by the maximum error E plays a crucial role. If data points outside the block constrained by E align with the regression trend of the points within the block, the approximation remains accurate. However, there might be situations where data points outside the block behave significantly differently from those within the block. In such cases, as clearly shown in Fig. 7b, this could lead to a less accurate linear regression in PRA, resulting in $E < E'$. This means that PRA has a lower performance than PLA in such scenarios. In some rare cases, all elements in \mathcal{E} (Algorithm 3), denoted as E' for each segment, are equivalent to E . In such scenarios, both algorithms exhibit identical last-mile search performance.

D. Serialize and Deserialize Models

After training, the LI models are serialized and stored in a metadata block called the Meta Index Block (see Fig. 3). This process involves traversing the model tree structure via depth-first search (DFS), serializing each node byte-by-byte. During deserialization, the model reconstructs the tree by determining the type of each node (leaf or internal) and populating the corresponding data structure.

The learned indices generally outperform the binary search in terms of time complexity. Therefore, the size of the set of stored nodes for model approximation is smaller than $O(\log N)$ when reading, while writing the entire dataset takes $O(N)$. As a result, the serialized model size is asymptotically negligible (see § IV-D). In practice, RocksDB writes occur in the background flush and compaction process, and since the

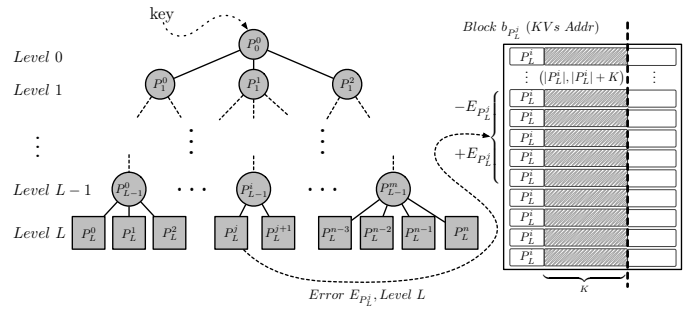


Fig. 8: Last-mile Search Optimization Flow

model is deserialized only once, overall read performance is significantly improved (see §IV-B1).

E. Last-mile Search Optimization

The final phase of the search process involves the last-mile search of the recovered block from storage (step ⑨ in Fig. 5). As illustrated in Fig. 1c, this step accounts for more than 40% of the indexing latency in RocksDB. Fig. 8 shows how DobLIX optimizes its performance by restoring data from the LI model computation trajectory (step ⑤ in Fig. 5) to improve the last-mile search process. Initially, the target key is searched within the string LI structure, as explained in § II-B. The LI model in DobLIX subsequently provides: (1) $Block\ b_{P_L^j}$: The block containing the target KV pair. (2) $M(\cdot)$: The LI estimation of the target KV pair index in $KVsAddr$ (Fig. 5). (3) $Level\ L$: The level at which the target key was found in the LI model. (4) $Error\ E_{P_L^j}$: The maximum range required to search for the target KV pair.

Optimizing Search Range. As described in § III-B, DobLIX necessitates a coordinate transformation to adapt the model output ($M(\cdot)$) for indexing on the retrieved block ($b_{P_L^j}$). This is achieved by deducting the count of keys in the previous blocks (maintained as the parameter “offset” in the metadata of the block introduced in Algs. 1 & 2):

$$I_{KV}(\cdot) = M_{adj}(\cdot) = M(\cdot) - b_{P_L^j}.offset$$

To better illustrate the adjustment, we consider SST_j in Fig. 2, in which the model is trained on the whole SSTable indexes. However, using the above adjustment, the coordination of model output for our solution (i.e., Fig. 2d) is transformed to the retrieved block B_2 .

Subsequently, DobLIX performs a binary search within the specified model error range $E_{P_L^j}$ on $M_{adj}(\cdot)$. This error range can be less than the maximum error E if a spline in the PLA method reaches the maximum block size B_{max} . In such cases, DobLIX calculates the spline error and incorporates it into the model, transmitting this information to the last-mile search process to streamline the number of key comparisons.

Optimizing String Comparison. DobLIX further optimizes the comparisons by avoiding full key comparisons. DobLIX provides the node level where the key is found in its string-LI structure. This level in the tree indicates the common prefix string, P_L^j , in the key (Fig. 8). Then DobLIX can ignore this common prefix, as all keys within the retrieved block share the same prefix. Additionally, DobLIX only compares string keys

up to their K bytes, ensuring that the key can be identified by comparing only the K byte following the prefix within the error range. Given that K generally consists of 8 or 16 bytes as explained in § II-B2 for shifts from demanding string comparisons to numerical comparisons.

F. Tuning Agent

DoBLIX employs Q-learning [49], a lightweight reinforcement learning (RL) algorithm [38], to dynamically fine-tune the LI and data access parameters. DoBLIX determines three key parameters in the creation of SSTables and the training model: (1) The choice between using the PLA vs. the PRA. (2) The maximum error of the LI in the PLA method (E), and (3) The maximum size of a block (B_{max}).

The state space for the Q-learning agent comprises the index model (PLA with error values ranging from 32 to 256, doubling at each step, and PRA, resulting in 5 distinct values), and the block size (4KB to 32KB, doubling at each step, yielding 4 distinct values, as recommended by RocksDB). This creates a total of 20 possible states. The action space consists of five actions: incrementing, decrementing, or maintaining the current value of the model error and block size.

The RL agent policy for exploring the feasible space is also guided by our optimization method (§ III-C1). It prioritizes block size over the approximation error. The policy evaluates the relationship between data block size and its load latency, identifying the first block size that alters this relationship (e.g. $O(\log N)$ to $O(N)$) as the upper bound. This effectively reduces the feasible space for exploration by limiting larger block sizes.

The reward function is defined below to consider both system latency and index storage: $R(s, a) = -\nu \cdot \text{Norm}(\text{AVG}(\text{latency})) - (1 - \nu) \cdot \text{Norm}(\text{AVG}(\text{index size}))$. This reward function is calculated as the negative sum of the normalized average latency and the normalized average of SSTables index size. We use sigmoid normalization to ensure that both latency and index size contribute to the reward on a comparable scale. The weighting parameter ν controls the relative importance of latency and index size in determining the overall reward (evaluated in § IV-F). In our experiments, we set ν as 1 to achieve the lowest latency; however, in some scenarios, storage may be more critical than can be set by lower values of ν .

Algorithm 4 outlines the agent tuning and execution process. The learning procedure begins by configuring the RL hyperparameters: α denotes the learning rate, while γ signifies the discount factor that balances immediate and future rewards. An epsilon decay strategy is used by initially setting a high exploration rate (ϵ) to investigate various actions, gradually lowering this value in successive iterations to exploit the optimal actions. At every 20 SSTables creation, the following steps occur: First, the agent obtains the average latency of the reads that have reached this level, as well as the index size of the previously created SSTable. Then, it measures the reward and updates it for the chosen action in the previous state. The agent then gets the available actions at that state.

Algorithm 4: System Tuning Agent

```

1  $Q \leftarrow \text{initializeQTable}()$ 
2  $\alpha, \gamma, \epsilon \leftarrow \text{initializeVariables}()$ 
3 while do
4   Fetch state  $s_{t-1}$ 
5    $L_t, I_t \leftarrow \text{fetchAverageLatencyAndSSTableIndexSize}()$ 
6    $R_t \leftarrow \text{calculateReward}(L_t, I_t)$ 
7   Observe state  $s_t$ 
8    $a' \leftarrow \arg \max_{a \in \text{Actions}} Q(s_t, a)$ 
9    $Q(s_{t-1}, a_{t-1}) \leftarrow$ 
      $(1 - \alpha)Q(s_{t-1}, a_{t-1}) + \alpha(R_t + \gamma Q(s_t, a'))$ 
10   $A_t \leftarrow \text{getAvailableActions}(s_t)$ 
11  if  $\text{generateRandNumber}() < \epsilon$  then
12     $a_t \leftarrow \text{getRandomAction}(A_t)$ 
13  else
14     $a_t \leftarrow \arg \max_{a \in A_t} Q(s_t, a)$ 
15   $\text{tuneSystem}(a_t)$ 
16   $s_t \leftarrow s_{t+1}$ 
17   $\epsilon \leftarrow \text{updateEpsilon}(\epsilon)$ 

```

Then, depending on the value of ϵ , the agent explores a new action or chooses the best action from the Q-table. In addition, we implement a reset mechanism for the RL agent that reverts ϵ to its initial value if the distribution undergoes a significant change. This ensures optimal exploration of the space under the new conditions.

IV. EVALUATIONS

This section presents the results of the DoBLIX evaluation, emphasizing its advantages over current leading methods. We design the evaluations to answer the following questions: 1. What performance advantages does DoBLIX offer? (§ IV-B) 2. How does the length of key-value pairs affect DoBLIX and other baseline systems? (§ IV-C) 3. What advantages do DoBLIX provide in the storage footprint? (§ IV-D) 4. How does the RL agent adjust its underlying parameters? (§ IV-F)

A. Experimental Setup

1) **Environment:** We implemented DoBLIX in C++17 and integrated it with RocksDB version 8.1.1. The source files were compiled with GCC 9.4.0. We conducted our evaluation on a Linux machine running Ubuntu 20.04, powered by an AMD Ryzen ThreadRipper Pro 5995WX processor with 64 cores at 2.7GHz and equipped with 256GB of DDR4 RAM. The storage device used was a SAMSUNG 980 Pro 2TB M.2 NVMe SSD. This NVMe SSD offers fundamental read and write performance measures as follows: sequential read speeds of 7,000 MB/s, random read speeds of 1,237K IOPS, sequential write speeds of 5,000 MB/s, and random write speeds of 172.5K IOPS. A single experiment was performed on a Seagate BarraCuda 4TB SATA SSD. We allocate 4 background threads to RocksDB, and set the “max_background_compactions” and “max_background_flushes” options as 4.

2) **Datasets:** We utilize four real-world datasets sourced from the Search on Sorted Data Benchmark (SOSD) [26] along with two synthetic datasets for evaluating DoBLIX. These datasets have been used in previous studies [15], [16],

[36]. Each contains 64 million key-value pairs. The size of the key and the value are set according to the experiments used in our baselines ([15], [36]) as 8 byte and 64 byte. We also conduct experiments with other fixed key and value sizes, and also with varying key and value sizes to reflect real-world applications. The following sections provide specific information about each dataset. *WIKI* [4]. Edit timestamps for Wikipedia articles. *AMZN*: Popularity of book sales collected from Amazon. *FB* [2]: An upsampled version of a Facebook user ID dataset. *OSM* [3]: Uniformly sampled locations as Google CellIds. *LOGN*: This synthetic dataset is generated from a lognormal distribution with parameters $\mu = 0$ and $\sigma = 2$, multiplied by 10^9 and rounded down to the nearest integer. *UNI*: This synthetic dataset is generated from a uniform distribution ranging from zero to 10^{16} .

3) **Workloads**: We evaluate `DobLIX` with four different workloads, each consisting of 10 million operations. *Read-Only*: Focuses solely on read operations. *Read-Heavy*: Emphasizes reads (90%) with a smaller proportion of inserts (10%). *Write-Heavy*: Involves an equal split between reads and inserts (50% each). *Write-Only*: Concentrates entirely on write operations. We also use YCSB [13] real benchmarks to evaluate `DobLIX`. In all workloads, the search key is selected randomly from the existing set of keys in the index with a Zipfian distribution [14], unless a different request distribution is specified.

4) **Baselines**: We select the following representative schemes as baselines for comparison. *RocksDB* [17]: An embedded high-performance KV-store used as the storage engine. We utilize the default indexing mechanism of RocksDB. *Bourbon* [15]: A KV store with an LI that accelerates lookups by understanding the distribution of keys. Based on WiscKey [37], a LevelDB [1] variant, Bourbon retains fixed block sizes, but might need to load several blocks (See Fig. 2A). The Bourbon source code is publicly accessible [5]. We incorporate Bourbon indexing method into our RocksDB configuration. *TridentKV* [36]: an LI variant of RocksDB that aims to retrieve KV pairs by loading only one data block. TridentKV modifies the size of the data blocks, potentially significantly increasing the size of the block, which can affect the lookup performance when loading a large block (see Fig. 2C). TridentKV code is available as open-source [6] and is built on top of RocksDB. We adopt their implementation in our evaluations.

5) **Metrics**: We use the following metrics to evaluate `DobLIX` and all other baselines. **Throughput**: Average rate of operations per second. **Latency**: Average latency in the 99th percentile of all operations. **Tail Latency**: The average latency of the 5% slowest operations. **Index size**: LI and index block size. **SSTable Compaction time**: The average duration taken to create SSTables in the compaction process.

6) **Parameters**: By default, all methods adhere to the default configuration settings of RocksDB. The default configurations of Bourbon and TridentKV are also employed. For certain parameters such as the chosen learning method (either PLA or PRA), the maximum error bound, and the maximum block size, the tuning agent is responsible for making decisions. Initially,

we use a 1% sample from the datasets to train this agent, after which we incorporate the agent into the system. In the case of the PLA method, we use the same setup as RSS [41] to configure a dynamic radix table with 18 bits for the first level, 12 bits for the second level and 8 bits for the third level and beyond.

Regarding the hyperparameters of the RL agent α and γ (see § III-F), we perform a sensitivity test with values 0.2, 0.5 and 0.8. We observe that optimal results are achieved by assigning a low value of 0.2 to α and a high value of 0.8 to γ . We also set the initial value of ϵ at 0.99, with its minimum value being 0.02, allowing for a low exploration rate even after the training period (§ IV-F). We set ν in the reward function as 1 to optimize solely on performance.

B. Performance

In this section, we detail a set of experiments designed to evaluate `DobLIX` performance, alongside a comparison with baseline systems. Importantly, no cache was integrated into any system, ensuring that the comparisons remain fair. The initial experiment (§ IV-B1) highlights that `DobLIX` improves throughput by up to 1.41 \times , 1.52 \times , and 2.21 \times relative to TridentKV, Bourbon, and RocksDB, respectively. In the second experiment (§ IV-B2), `DobLIX` achieves up to 2.67 \times better throughput in terms of tail latency. The third experiment (§ IV-B3) examines the optimization of `DobLIX` lookup latency components. The fourth experiment (§ IV-B4) showcases `DobLIX` enhanced performance on the realistic YCSB macrobenchmarks. Finally, the last experiment (§ IV-B5) demonstrates `DobLIX` performance across varying request distributions.

1) **Throughput: Read-Only Workload**. Fig. 9a displays the throughput when subjected to a read-only workload on different datasets. In this scenario, `DobLIX` achieves the highest throughput, reaching a maximum of 105K *ops/sec* with the LOGN dataset. Compared to TridentKV, Bourbon, and RocksDB, `DobLIX` increases the average throughput by 1.41 \times , 1.57 \times , and 1.92 \times , respectively.

Read-Heavy Workload. Fig. 9b displays the performance results under the read-heavy workload, where there is a minor write rate. `DobLIX` continues to show the highest throughput in all datasets, reaching up to 82K *ops/sec*. Compared to TridentKV, Bourbon, and RocksDB, `DobLIX` increases the average throughput by 1.27 \times , 1.36 \times , and 1.22 \times , respectively. Despite the marginal reduction in throughput from write operations due to the slight training overhead for new SSTables, `DobLIX` and other LIs still maintain superior throughput compared to RocksDB indexing approach.

Balanced Workload. In this workload with increased write operations, `DobLIX` continues to outperform other systems in terms of throughput. As depicted in Fig. 9c, `DobLIX` achieves an average improvement of 1.29 \times , 1.27 \times , and 1.31 \times compared to TridentKV, Bourbon, and RocksDB, respectively.

Write-Heavy Workload. In Fig. 9d, we show data from a write-heavy workload scenario, representing the maximum write rate observed in our experiments. Once again, `DobLIX` shows

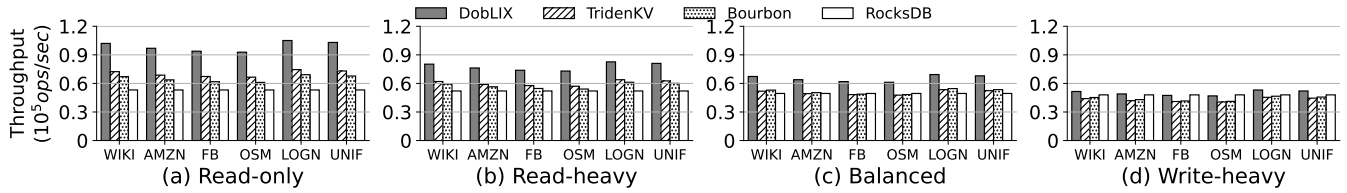


Fig. 9: Throughput Comparison.

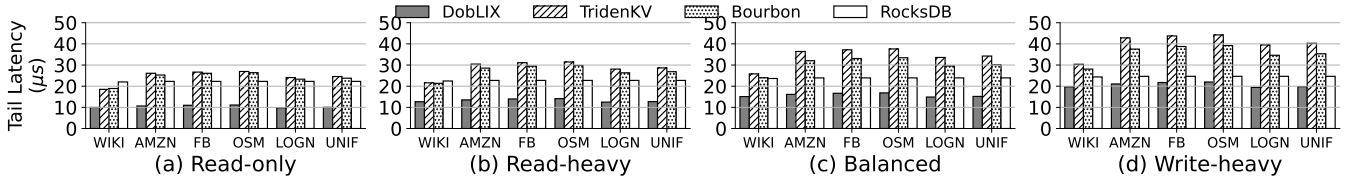


Fig. 10: Tail Latency Comparison.

the highest throughput, reaching $53K$ ops/sec. Compared to TridentKV, Bourbon, and RocksDB, *DobLIX* increases the average throughput by $1.16\times$, $1.14\times$, and $1.04\times$, respectively.

Takeaway: *DobLIX* optimization enhances the throughput of the index and data access phase. By optimizing data access, *DobLIX* minimizes read amplification by ensuring that only one block is precisely read per query while maintaining optimal block sizes. In contrast, Bourbon loads multiple blocks per lookup, and TridentKV features excessively large block sizes. When handling write-heavy tasks, *DobLIX* outperforms Bourbon and TridentKV by minimizing write amplification through its smaller index size. Additionally, *DobLIX* enhancements in read queries make it slightly superior to RocksDB, even in scenarios with heavy write operations which the reason is explained in § III-D.

2) **Tail Latency:** Analyzing tail latencies of different methods is vital because it defines the performance expectations for users and applications regarding their back-end key-value storage engine under the most challenging scenarios.

Read-Only Workload. Fig. 10a shows the tail latency results for read-only workloads, indicating that *DobLIX* exhibits the lowest tail latency. Notably, *DobLIX* improvement in tail latency surpasses the improvements observed in throughput. Compared to TridentKV, Bourbon, and RocksDB, *DobLIX* achieves improvements of $1.85\times$, $1.89\times$, and $2.13\times$, respectively. This difference is due to the high read amplification and index lookup inefficiency of other methods, explained in § IV-B.

Workloads with Write. Fig. 10{b,c,d} presents the tail latency results for read-heavy, balanced, and write-heavy workloads. These figures illustrate that *DobLIX* achieves the lowest tail latency across all workload types. In terms of tail latency, RocksDB indexing outperforms both Bourbon and TridentKV, which employ Lling without optimizing for the data access phase. TridentKV exhibits the highest tail latency among these workloads, showing up to $2.67\times$ greater latency than *DobLIX* due to its large blocks, which negatively affect both read and write operations. Bourbon also experiences elevated tail latency in write-intensive workloads due to its dependence on a garbage collection mechanism [15], which degrades its performance

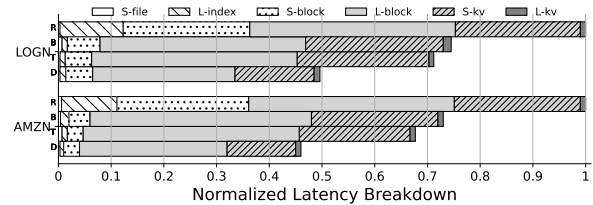


Fig. 11: Normalized Latency Breakdown of *DobLIX* (‘D’), TridentKV(‘T’), Bourbon(‘B’), and RocksDB (‘R’). ‘L’ and ‘S’, on the legend, stand for load and seek, respectively.

during this period.

Takeaway: The result shows that *DobLIX* has lower latency spikes while competing with its opponents in the ordinary time span.

3) **Lookup Query Latency Breakdown:** In Fig. 11, the breakdown of the latencies of systems in read-heavy workloads is presented using the AMZN and LOGN datasets. Latencies are normalized by RocksDB latency. *DobLIX* achieves average latency improvements of up to 23%, 27%, and 56% compared to TridentKV, Bourbon, and RocksDB. Certain components, such as the Seek file or I_{SST} (S-file) and Load KV (L-KV), show minimal changes, as these steps are consistent across all methods. The load index block (L-index) sees an improvement of 10.35% on average compared to RocksDB, attributed to *DobLIX* LI methods. *DobLIX* also improves the lookup of blocks or $I_{IndexBlock}$ (S-block) by up to 22% compared to RocksDB. Significant enhancements compared to Bourbon and TridentKV are seen in block loading (L-block) and locating the target KV within the block or I_{KV} (S-KV). *DobLIX* multi-objective optimization strategy targets block size and precise block retrieval, resulting in a decrease in average block loading time by as much as 12.2% compared to other methods. In terms of the KV last-mile search (S-KV), *DobLIX* demonstrates an average reduction of 11.1% due to two optimizations: the elimination of key prefixes and the narrowing of the error bound range (as discussed in § III-E).

4) **YCSB Macrobenchmarks:** Fig. 12a illustrates the throughput performance of *DobLIX* and the three baseline systems on various YCSB workloads. In particular, *DobLIX* consistently achieves the highest throughput on the six workloads. In the read-heavy YCSB{B,C,D} workloads,

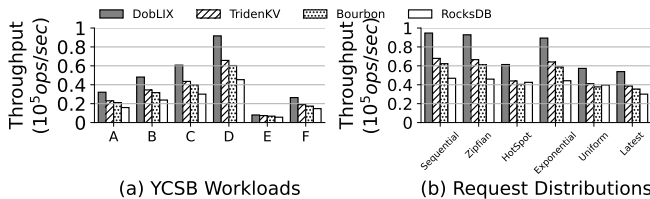


Fig. 12: Throughput Comparison on YCSB macrobenchmarks and various distribution workloads.

DobLIX demonstrates superior throughput of 481K, 607K, and 916K ops/sec, respectively. On average, DobLIX increases throughput by 1.32 \times , 1.42 \times , and 2.02 \times compared to TridentKV, Bourbon, and RocksDB, respectively. For balanced workloads YCSB{A,F}, DobLIX reaches throughput levels of 320K and 264K ops/sec, respectively, outperforming other techniques with an average increase in throughput of 56%. In the YCSB-E scan-focused benchmark, DobLIX achieves the highest throughput of 80K operations per second. However, its gains over TridentKV, Bourbon, and RocksDB are relatively modest at 9.2%, 16.7%, and 42.8%, respectively. This relative performance is because the LIs enhance point queries rather than scan operations. During the scan phase of the range queries, all techniques exhibit uniform performance.

5) *Various Request Distributions*: Fig. 12b shows the throughput of DobLIX and the three baselines in read-only workloads in the OSM dataset on six different request distributions. The figure shows that DobLIX maintains its superior read performance in the six request distributions. On average, DobLIX achieves 39.4%, 52.1%, and 78.9% higher throughput compared to TridentKV, Bourbon, and RocksDB.

C. Impact of Key and Value Length

In the previous section, we evaluated DobLIX performance with fixed 8-byte keys and 64-byte values. Here, we first show DobLIX performance by changing the key and value sizes while maintaining their constancy during the experiments. Then, we perform more realistic experiments in which the key and value sizes vary within each experiment (see § II-C).

1) *Fixed-sized key-values*: Fig. 13a shows the impact of different fixed key sizes on each method. We excluded Bourbon from this experiment because of its limitation to 8-byte keys. The results of the OSM dataset with read-only workload show that DobLIX has the highest throughput, even as the key size increases due to its efficiency in removing the key prefixes and locating the block and target key value. However, TridentKV throughput drops drastically due to creating large block sizes by increasing the key size. The performance gap between DobLIX and RocksDB narrows with increasing size, as larger key-value (KV) loads impact both methods. Fig. 13b shows the impact of various fixed value sizes on throughput. The results show that DobLIX has the highest throughput up to a value of 1KB. For the value size 4KB, Bourbon works better as it disaggregates keys and values, which is efficient for large value sizes.

2) *Variable-sized key-values*: In this section, we conduct practical experiments utilizing variable KV sizes. We used the

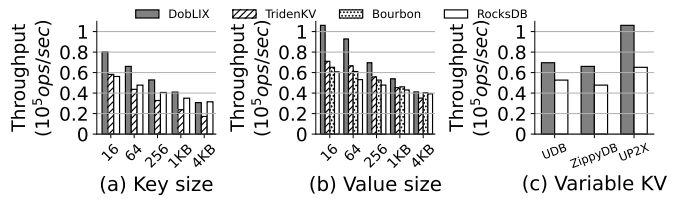


Fig. 13: Impact of various key-value sizes.

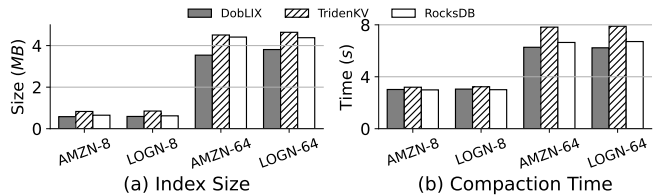


Fig. 14: Average index size and SSTable creation time.

mean and standard deviations of the KVs of three RocksDB applications (see § II-C). As none of the previously established index methods can manage variable KVs, our comparison is exclusively with RocksDB. Fig. 13c shows the experimental results for these KV sizes. It illustrates that DobLIX functions effectively with variable key-value sizes and achieves 1.32 \times , 1.38 \times , and 1.62 \times in key-value sizes such as UDB, ZippyDB, and UP2X.

D. Storage Footprint

Fig. 14a shows the index size for the AMZN and LOGN datasets with 8- and 64-byte key sizes. We omit Bourbon as it only works with 8-byte numerical keys. The index block for each method will be written to storage beside the actual key values, hence index size has a direct relation with space and write amplification. The figure shows that in 8-byte keys, the index size of DobLIX and RocksDB has a negligible difference, while both are less than TridentKV. However, for 64-byte keys, DobLIX improves indexing by 25.9% on average. This is because DobLIX removes the longest common prefix from each cluster of keys on each node (see § III-E), and each node only keeps 8-byte numerical data. This shows that DobLIX has the lowest index size, and since it does not add any other data except the serialized LI model, it has the lowest write and space amplification compared to other methods.

E. Compaction Time

In DobLIX and other baselines, SSTables are constructed in the background flush and compaction processes [52]. Fig. 14b demonstrates the average compaction time to build SSTables on the four different workloads and datasets mentioned in § IV-D. The data indicate that the DobLIX LI model does not add overhead during the SSTable construction compared to RocksDB. Notably, with 64-byte keys, DobLIX construction time is 5.9% shorter than RocksDB, due to the smaller index size of DobLIX. Additionally, compared to TridentKV, DobLIX reduces construction time by 24.7%, attributed to TridentKV lack of prefix removal optimization in its string model. Specifically, DobLIX average SSTable construction time for 64-byte keys is 6.2 seconds, with model training taking 302 ms (4.8% of the total time) and serialization and metadata

writing taking 237 ms (3.7% of the total time). In contrast, TridentKV model training time is 817 ms, and serialization plus metadata writing time is 414 ms.

F. Parameter Tuning

In this section, we present the results of the RL agent for parameter tuning and analyze the impact of parameters on throughput and total index size. The evaluation uses the AMZN dataset under two read-heavy workloads: (1) point-query with a Zipfian distribution, and (2) range queries over 100 consecutive KV pairs with a uniform distribution. We also vary the ν parameter in the RL reward function (§III-F) between 0 and 1 to evaluate trade-offs between index storage footprint and throughput optimization. The left side of Fig. 15 illustrates throughput between two RL episodes (each episode is executed after 20 SST creation) and the estimated total index size after each episode. The index size is estimated using a linear approximation based on current keys added to a total of 64 million keys in the dataset. The right side of the figure displays the RL agent Q-table rewards, highlighting the best parameter configurations for each workload.

Throughput Optimization. For point queries (Fig. 15a), the throughput increases from 45K to 93K ops/sec after 50 episodes. This improvement is achieved by tuning parameters to prioritize throughput at the cost of increasing storage size. The heatmap shows that smaller block sizes yield higher rewards because they reduce read amplification, minimizing the size of the retrieved block per query. Among the index models, PLA with a maximum error of 128 achieves the best performance. A smaller error increases the block count, while a larger error (i.e., 256) raises the cost of intra-block last-mile searches.

For range queries (Fig. 15c), parameter rewards are less sensitive compared to point queries since range query performance is dominated by sequential KV iteration. However, a block size of 16KB paired with the PRA model achieves the highest reward. This size strikes a balance, being more efficient than 8KB since the data being read is more than 8KB, so reading 16KB blocks lowers the amount of metadata reads. Additionally, the PRA model outperforms PLA with different error ranges at the 16KB block size, as this specific setting has a characteristic similar to Fig. 7b where $E' < E$.

Storage Optimization. Fig.15b and Fig.15d show results when the RL agent prioritizes minimizing the index size. The heatmaps indicate that the trends for both workloads are similar, as the stored data index is identical. Larger block sizes consistently reduce the index size by decreasing the number of blocks and associated metadata. Among the index models, PLA with a maximum error of 256 achieves the highest reward by reducing the number of splines, thus minimizing the index overhead. In both workloads, the chosen parameters achieve an estimated index size of less than 500MB, which is half of the index size when the optimization is on the throughput.

DobLIX Limitation. This experiment on the RL agent shows that DobLIX requires at least 50 RL episodes to find near-optimal parameters that satisfy the throughput and storage

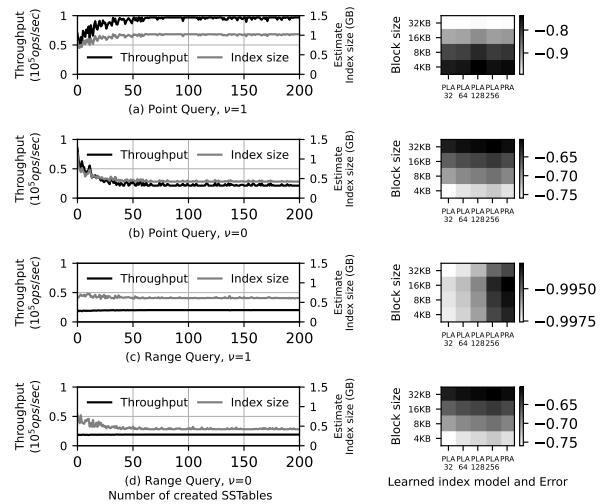


Fig. 15: RL agent parameter tuning. Each row shows two plots for one specific workload and reward parameter, The right plot shows the improvement in the throughput and estimated index size during the workload. The left plot shows the reward heatmap at the end of the experiment. Darker colors have higher rewards.

goals. One possible future work is to reduce the cold start caused by the RL agent and speed up the exploration time.

V. RELATED WORK

The read performance of LSM-tree is compromised due to its multilayer structure. Research has focused on optimizing it through three main strategies: filter optimization, cache optimization, and index optimization. (1) *Filter Optimization.* Several works utilize filters to skip unnecessary reading since the filters do not return a false negative [33], [44]. However, the filters suffer from high false positive rates and excessive memory usage. (2) *Cache Optimization.* LSbM-tree [43] adds a buffer to minimize cache invalidations due to compactions. AC-Key [50] introduces an adaptive caching algorithm to adjust the cache size based on the workload. Although caching accelerates the lookup of recently accessed data, it consumes significant storage as the cache size increases. (3) *Index Optimization.* SLM-DB [25] implemented a persistent global B+tree index on NVM, and Kvell [31] adopts various memory index structures. Several studies [15], [36], [47] also built an LI using static data stored in SSTables to speed up read queries on SSTables. However, these studies aim to improve indexing without considering their system adjustment on the data access part for data retrieval from persistent memory.

VI. CONCLUSION

DobLIX presents a novel index architecture for LSM-trees, enhancing both indexing efficiency and data retrieval. We show that DobLIX markedly increases throughput in RocksDB, a widely used LSM-tree-based KV store. Redesigning index optimization introduces new possibilities for system engineering. This innovative method, which addresses two specific goals, provides a new perspective on designing systems with multiple seemingly unrelated objectives. Future research will explore multi-objective optimization techniques that consider various parameter combinations concurrently.

REFERENCES

- [1] Leveldb. <https://opensource.googleblog.com/2011/07/leveldb-fast-persistent-key-value-store.html>, 2011.
- [2] Fb dataset. <https://doi.org/10.7910/DVN/JGVF9A/Y54S19>, 2019.
- [3] Osm dataset. <https://console.cloud.google.com/marketplace/product/openstreetmap/geo-openstreetmap>, 2019.
- [4] Wikits dataset. <https://doi.org/10.7910/DVN/JGVF9A/SVN8PI>, 2019.
- [5] Bourbon code. <https://github.com/edydfang/Bourbon>, 2020.
- [6] Tridentkv code. <https://github.com/emperorlu/Learned-RocksDB>, 2021.
- [7] ABERNETHY, J. D., SCHAPIRE, R., AND SYED, U. Lexicographic optimization: Algorithms and stability. In *International Conference on Artificial Intelligence and Statistics* (2024), PMLR, pp. 2503–2511.
- [8] BOYD, S., AND VANDENBERGHE, L. *Convex optimization*. Cambridge university press, 2004.
- [9] CAO, Z., DONG, S., VEMURI, S., AND DU, D. H. C. Characterizing, modeling, and benchmarking rocksdb key-value workloads at facebook. In *Proceedings of the 18th USENIX Conference on File and Storage Technologies* (USA, 2020), FAST’20, USENIX Association, p. 209–224.
- [10] CHANG, F., DEAN, J., GHEMAWAT, S., HSIEH, W. C., WALLACH, D. A., BURROWS, M., CHANDRA, T., FIKES, A., AND GRUBER, R. E. Bigtable: A distributed storage system for structured data. *ACM Transactions on Computer Systems (TOCS)* 26, 2 (2008), 1–26.
- [11] CHATTERJEE, S., PEKALA, M. F., KRUGLYAK, L., AND IDREOS, S. Limousine: Blending learned and classical indexes to self-design larger-than-memory cloud storage engines. *Proceedings of the ACM on Management of Data* 2, 1 (2024), 1–28.
- [12] CHINCHULUUN, A., AND PARDALOS, P. M. A survey of recent developments in multiobjective optimization. *Annals of Operations Research* 154, 1 (2007), 29–50.
- [13] COOPER, B. F., SILBERSTEIN, A., TAM, E., RAMAKRISHNAN, R., AND SEARS, R. Benchmarking cloud serving systems with ycsb. In *Proceedings of the 1st ACM Symposium on Cloud Computing* (New York, NY, USA, 2010), SoCC ’10, ACM, pp. 143–154.
- [14] CORMODE, G., AND HADJIELEFTHERIOU, M. Finding frequent items in data streams. *Proceedings of the VLDB Endowment* 1, 2 (2008), 1530–1541.
- [15] DAI, Y., XU, Y., GANESAN, A., ALAGAPPAN, R., KROTH, B., ARPACI-DUSSEAU, A. C., AND ARPACI-DUSSEAU, R. H. From wisckey to bourbon: a learned index for log-structured merge trees. In *Proceedings of the 14th USENIX Conference on Operating Systems Design and Implementation* (USA, 2020), OSDI’20, USENIX Association.
- [16] DING, J., MINHAS, U. F., YU, J., WANG, C., DO, J., LI, Y., ZHANG, H., CHANDRAMOULI, B., GEHRKE, J., KOSSMANN, D., ET AL. Alex: an updatable adaptive learned index. *SIGMOD*.
- [17] DONG, S., KRYCZKA, A., JIN, Y., AND STUMM, M. Evolution of development priorities in key-value stores serving large-scale applications: The RocksDB experience. In *19th USENIX Conference on File and Storage Technologies (FAST 21)* (Feb. 2021), USENIX Association, pp. 33–49.
- [18] FERRAGINA, P., AND VINCIGUERRA, G. The pgm-index: a fully-dynamic compressed learned index with provable worst-case bounds. *VLDB* 13, 8 (2020).
- [19] GALAKATOS, A., MARKOVITCH, M., BINNIG, C., FONSECA, R., AND KRASKA, T. Fiting-tree: A data-aware index structure. In *SIGMOD* (2019).
- [20] HEIDARI, A., AHMADI, A., AND ZHANG, W. Uplif: An updatable self-tuning learned index framework. *arXiv preprint arXiv:2408.04113* (2024).
- [21] HEIDARI, A., AHMADI, A., ZHI, Z., AND ZHANG, W. Metahive: A cache-optimized metadata management for heterogeneous key-value stores. *Proceedings of the VLDB Endowment*. ISSN 2150, 8097.
- [22] HEIDARI, A., KUSHAGRA, S., AND ILYAS, I. F. On sampling from data with duplicate records. *arXiv preprint arXiv:2008.10549* (2020).
- [23] HEIDARI, A., MCGRATH, J., ILYAS, I. F., AND REKATSINAS, T. Holodetect: Few-shot learning for error detection. In *Proceedings of the 2019 International Conference on Management of Data* (2019), pp. 829–846.
- [24] HEIDARI, A., MICHALOPOULOS, G., ILYAS, I. F., AND REKATSINAS, T. Record fusion via inference and data augmentation. *ACM/JMS Journal of Data Science* 1, 1 (2024), 1–23.
- [25] KAIYRAKHMET, O., LEE, S., NAM, B., NOH, S. H., AND CHOI, Y.-R. {SLM-DB}:: {Single-Level} {Key-Value} store with persistent memory. In *17th USENIX Conference on File and Storage Technologies (FAST 19)* (2019), pp. 191–205.
- [26] KIPF, A., MARCUS, R., VAN RENEN, A., STOIAN, M., KEMPER, A., KRASKA, T., AND NEUMANN, T. Sosd: A benchmark for learned indexes. *arXiv preprint arXiv:1911.13014* (2019).
- [27] KIPF, A., MARCUS, R., VAN RENEN, A., STOIAN, M., KEMPER, A., KRASKA, T., AND NEUMANN, T. Radixspline: a single-pass learned index. In *Proceedings of the third international workshop on exploiting artificial intelligence techniques for data management* (2020), pp. 1–5.
- [28] KRASKA, T., BEUTEL, A., CHI, E. H., DEAN, J., AND POLYZOTIS, N. The case for learned index structures. In *SIGMOD* (2018).
- [29] LAKSHMAN, A., AND MALIK, P. Cassandra: a decentralized structured storage system. *ACM SIGOPS operating systems review* 44, 2 (2010), 35–40.
- [30] LAN, H., BAO, Z., CULPEPPER, J. S., AND BOROVICA-GAJIC, R. Updatable learned indexes meet disk-resident dbms - from evaluations to design choices. *Proc. ACM Manag. Data* 1, 2 (jun 2023).
- [31] LEPERS, B., BALMAU, O., GUPTA, K., AND ZWAENPOEL, W. Kvell: the design and implementation of a fast persistent key-value store. In *Proceedings of the 27th ACM Symposium on Operating Systems Principles* (2019), pp. 447–461.
- [32] LI, P., LU, H., ZHENG, Q., YANG, L., AND PAN, G. Lisa: A learned index structure for spatial data. In *Proceedings of the 2020 ACM SIGMOD international conference on management of data* (2020), pp. 2119–2133.
- [33] LI, Y., TIAN, C., GUO, F., LI, C., AND XU, Y. {ElasticBF}: Elastic bloom filter with hotness awareness for boosting read performance in large {Key-Value} stores. In *2019 USENIX Annual Technical Conference (USENIX ATC 19)* (2019), pp. 739–752.
- [34] LIVSHITS, E., HEIDARI, A., ILYAS, I. F., AND KIMELFELD, B. Approximate denial constraints. *arXiv preprint arXiv:2005.08540* (2020).
- [35] LU, B., DING, J., LO, E., MINHAS, U. F., AND WANG, T. Apex: a high-performance learned index on persistent memory. *Proc. VLDB Endow.* 15, 3 (nov 2021), 597–610.
- [36] LU, K., ZHAO, N., WAN, J., FEI, C., ZHAO, W., AND DENG, T. Tridentkv: A read-optimized lsm-tree based kv store via adaptive indexing and space-efficient partitioning. *IEEE Transactions on Parallel and Distributed Systems* 33, 8 (2022), 1953–1966.
- [37] LU, L., PILLAI, T. S., GOPALAKRISHNAN, H., ARPACI-DUSSEAU, A. C., AND ARPACI-DUSSEAU, R. H. Wisckey: Separating keys from values in ssd-conscious storage. *ACM Transactions On Storage (TOS)* 13, 1 (2017), 1–28.
- [38] MO, D., CHEN, F., LUO, S., AND SHAN, C. Learning to optimize lsm-trees: Towards a reinforcement learning based key-value store for dynamic workloads. *Proceedings of the ACM on Management of Data* 1, 3 (2023), 1–25.
- [39] MOZAFARI, B., GOH, E. Z. Y., AND YOON, D. Y. Cliffguard: A principled framework for finding robust database designs. In *Proceedings of the 2015 ACM SIGMOD International Conference on Management of Data* (New York, NY, USA, 2015), SIGMOD ’15, Association for Computing Machinery, p. 1167–1182.
- [40] SABEK, I., AND KRASKA, T. The case for learned in-memory joins.
- [41] SPECTOR, B., KIPF, A., VAIDYA, K., WANG, C., MINHAS, U. F., AND KRASKA, T. Bounding the last mile: Efficient learned string indexing. *arXiv preprint arXiv:2111.14905* (2021).
- [42] TANG, C., WANG, Y., DONG, Z., HU, G., WANG, Z., WANG, M., AND CHEN, H. Xindex: a scalable learned index for multicore data storage. In *Proceedings of the 25th ACM SIGPLAN symposium on principles and practice of parallel programming* (2020), pp. 308–320.
- [43] TENG, D., GUO, L., LEE, R., CHEN, F., MA, S., ZHANG, Y., AND ZHANG, X. Lsbm-tree: Re-enabling buffer caching in data management for mixed reads and writes. In *2017 IEEE 37th International Conference on Distributed Computing Systems (ICDCS)* (2017), IEEE, pp. 68–79.
- [44] WANG, H., GUO, T., YANG, J., AND ZHANG, H. Grf: A global range filter for lsm-trees with shape encoding. *Proceedings of the ACM on Management of Data* 2, 3 (2024), 1–27.
- [45] WANG, W., AND DU, D. H.-C. Learnedkv: Integrating lsm and learned index for superior performance on ssd. *arXiv preprint arXiv:2406.18892* (2024).
- [46] WANG, Y., TANG, C., WANG, Z., AND CHEN, H. Sindex: a scalable learned index for string keys. In *Proceedings of the 11th ACM SIGOPS Asia-Pacific Workshop on Systems* (2020), pp. 17–24.
- [47] WANG, Y., YUAN, J., WU, S., LIU, H., CHEN, J., MA, C., AND QIN, J. Leaderkv: Improving read performance of KV stores via learned index and decoupled KV table. In *40th IEEE International Conference on*

- Data Engineering, ICDE 2024, Utrecht, The Netherlands, May 13-16, 2024* (2024), IEEE, pp. 29–41.
- [48] WANG, Z., DING, C., SONG, F., LU, K., WAN, J., TAN, Z., XIE, C., AND LI, G. Wipe: A write-optimized learned index for persistent memory. *ACM Trans. Archit. Code Optim.* 21, 2 (feb 2024).
 - [49] WATKINS, C. J., AND DAYAN, P. Q-learning. *Machine learning* 8 (1992), 279–292.
 - [50] WU, F., YANG, M.-H., ZHANG, B., AND DU, D. H. {AC-Key}: Adaptive caching for {LSM-based}{Key-Value} stores. In *2020 USENIX Annual Technical Conference (USENIX ATC 20)* (2020), pp. 603–615.
 - [51] YANG, Y., AND CHEN, S. Lits: An optimized learned index for strings. *Proceedings of the VLDB Endowment* 17, 11 (2024), 3415–3427.
 - [52] YU, Q., GUO, C., ZHUANG, J., THAKKAR, V., WANG, J., AND CAO, Z. Caas-lsm: compaction-as-a-service for lsm-based key-value stores in storage disaggregated infrastructure. *Proceedings of the ACM on Management of Data* 2, 3 (2024), 1–28.
 - [53] ZHANG, J., SU, K., AND ZHANG, H. Making in-memory learned indexes efficient on disk. *Proc. ACM Manag. Data* 2, 3 (may 2024).